The Astrophysical Journal, 672:198–206, 2008 January 1

THE FAINT-END SLOPES OF GALAXY LUMINOSITY FUNCTIONS IN THE COSMOS FIELD[1]

Charles T. Liu,[2] Peter Capak,[3] Bahram Mobasher,[4] Timothy A. D. Paglione,[5] R. Michael Rich,[6]
Nicholas Z. Scoville,[3] Shana M. Tribiano,[7] and Neil D. Tyson[8]

Received 2006 August 11; accepted 2007 August 9

ABSTRACT

We examine the faint-end slope of the rest-frame *V*-band luminosity function (LF), with respect to galaxy spectral type, of field galaxies with redshift $z < 0.5$, using a sample of 80,820 galaxies with photometric redshifts in the 2 deg^2 Cosmic Evolution Survey (COSMOS) field. For all galaxy spectral types combined, the LF slope ranges from -1.24 to -1.12, from the lowest redshift bin to the highest. In the lowest redshift bin ($0.02 < z < 0.1$), where the magnitude limit is $M_V \lesssim -13$, the slope ranges from $\alpha \sim -1.1$ for galaxies with early-type spectral energy distributions (SEDs) to $\alpha \sim -1.9$ for galaxies with low-extinction starburst SEDs. In each galaxy SED category (early-type, Sbc, Scd+Irr, and starburst), the faint-end slopes grow shallower with increasing redshift; in the highest redshift bin ($0.4 < z < 0.5$), $\alpha \sim -0.5$ and -1.3 for early types and starbursts, respectively. The steepness of α at lower redshifts could be qualitatively explained by LF evolution, or by large numbers of faint dwarf galaxies, perhaps of low surface brightness, that are not detected at higher redshifts.

Subject headings: cosmology: observations — galaxies: dwarf — galaxies: evolution — galaxies: fundamental parameters — galaxies: luminosity function, mass function — surveys

Online material: color figure

1. INTRODUCTION

The luminosity function (LF) of galaxies varies substantially with respect to many key physical parameters such as galaxy morphology, environment, color, star formation rate, surface brightness, and redshift. These many differences serve as powerful diagnostics of the broad tapestry of galaxy evolution.

The most important requirement for the accurate derivation of galaxy LFs is large, complete samples of galaxies with reliable photometry and redshift determinations. The Cosmic Evolution Survey (COSMOS; Scoville et al. 2007a) contains not only the largest contiguous area of the sky yet observed with the *Hubble Space Telescope* (*HST*), but also deep multiwavelength imaging across the entire 2 deg^2 COSMOS field (Capak et al. 2007). COSMOS thus affords deep, homogeneous photometric and photometric redshift coverage for a sample of some 10^6 galaxies, complementing well at higher redshifts the largest galaxy surveys of the relatively nearby universe with which galaxy LFs have been derived, such as the Two Degree Field Galaxy Redshift Survey (2dFGRS; Colless et al. 2001; Croton et al. 2005) and the Sloan Digital Sky Survey (SDSS; Blanton et al. 2003; Bell et al. 2003; Abazajian et al. 2004).

Comprehensive analyses of the LF characteristics of the entire COSMOS galaxy sample will ultimately be forthcoming upon the completion of the spectroscopic portion of the survey (Lilly et al. 2007) and the continued addition and refinement of the photometric and photometric redshift measurements in multiple bandpasses (Capak et al. 2007; Mobasher et al. 2007). Already, however, it is feasible to address important scientific questions about galaxy LFs with the current optical and near-infrared multiband data (Capak et al. 2007; Taniguchi et al. 2007; Scarlata et al. 2007) in conjunction with the *HST* I_{814} broadband Advanced Camera for Surveys (ACS) imaging (Scoville et al. 2007b).

One particular component of the field galaxy LF, the faint end ($M_{AB} > -18$) of the LF at low to intermediate ($0 \lesssim z \lesssim 0.5$) redshifts, is uniquely well suited for analysis with the COSMOS data. This population of galaxies lies in an apparent magnitude range somewhat beyond the 2dFGRS and SDSS survey limits; they are too faint for spectroscopic observations and have redshifts too low to be included in surveys optimized for high-redshift galaxies. Yet exploring these galaxies' contribution to the overall LF is critical for understanding galaxy evolution during the latter half of cosmic history.

Recent comprehensive studies of field galaxy LF evolution have focused on the luminosity evolution of the bright end ($M_{AB} \lesssim -20$). There, some consensus appears to be gradually emerging about the extent of that evolution. Dahlen et al. (2005), Willmer et al. (2006), and Scarlata et al. (2007) all find a brightening of $M_{B,*}$ by $\sim$1 mag in the range $0 \lesssim z \lesssim 1$. In shorter wavelength

[1] Based on observations with the NASA/ESA *Hubble Space Telescope*, obtained at the Space Telescope Science Institute, which is operated by the Association of Universities for Research in Astronomy (AURA), Inc., under NASA contract NAS 5-26555; also based on data collected at Kitt Peak National Observatory, Cerro Tololo Inter-American Observatory, and the National Optical Astronomy Observatory, which are operated by AURA, Inc., under cooperative agreement with the National Science Foundation; at the Subaru Telescope, which is operated by the National Astronomical Observatory of Japan; with *XMM-Newton*, an ESA science mission with instruments and contributions directly funded by ESA Member States and NASA; at the European Southern Observatory under Large Program 175.A-0839, Chile; at the Canada-France-Hawaii Telescope with MegaPrime/MegaCam, operated as a joint project by the CFHT Corporation, CEA/DAPNIA, the National Research Council of Canada, the Canadian Astronomy Data Centre, the Centre National de la Recherche Scientifique de France, TERAPIX, and the University of Hawaii; and the National Radio Astronomy Observatory, which is a facility of the National Science Foundation operated under cooperative agreement by AURA, Inc.

[2] Astrophysical Observatory, Department of Engineering Science and Physics, City University of New York, College of Staten Island, 2800 Victory Boulevard, Staten Island, NY 10314.

[3] California Institute of Technology, MC 105-24, 1200 East California Boulevard, Pasadena, CA 91125.

[4] Space Telescope Science Institute, 3700 San Martin Drive, Baltimore, MD 21218.

[5] City University of New York, York College, 94-20 Guy R. Brewer Boulevard, Jamaica, NY 11451.

[6] Department of Physics and Astronomy, University of California, Los Angeles, CA 90095.

[7] City University of New York, Borough of Manhattan Community College, 199 Chambers Street, New York, NY 10007.

[8] American Museum of Natural History, Central Park West at 79th Street, New York, NY 10024.

bandpasses, the luminosity evolution is more pronounced, while at longer wavelengths it appears to be weaker and possibly even present in the negative sense, dimming in the near-infrared J band from $z \sim 0.4$ to 0.9 (Dahlen et al. 2005).

The evolution of the faint-end slope, however, remains highly uncertain. At low redshifts, results from the SDSS (Blanton et al. 2005; Baldry et al. 2005), the 2dFGRS (Croton et al. 2005), and other large data sets (see, e.g., Brown et al. 2001; Budavari et al. 2005; Driver et al. 2007) roughly agree, for example, on a moderate slope of $\alpha \sim -1.1$. Beyond redshifts of a few tenths, the faint-end slope becomes very difficult to address, mainly because the number of low-luminosity galaxies detected in galaxy surveys decreases dramatically with increasing redshift. Despite a number of efforts to measure evolution in the faint-end slope at redshifts less than $z \sim 1$ (Wolf et al. 2003; Ilbert et al. 2005; Zucca et al. 2006), very little is known for galaxies fainter than $M \sim -18$. This is in part because the relationship between the bright-end and faint-end characteristics of galaxy LFs is not straightforward, often resulting in a trade-off between the precision LF evolution measurements at the two ends. Baldry et al. (2005) and Willmer et al. (2006), for example, each select fixed LF faint-end slopes based on galaxies brighter than $M \sim -18$ and use that constraint throughout their bright-end evolution measurements.

Whether or not the faint-end slope evolves with redshift, however, it is clear that its steepness varies widely for galaxies of different morphological and spectral types, indicating substantial differences in the evolutionary histories of galaxies. Broadly speaking, irregular galaxies, "blue" galaxies, and strongly star-forming galaxies, three significantly overlapping galaxy subpopulations, evolve more strongly than galaxies of other types. Such galaxies are characterized by very steep faint-end LF slopes and substantial evolution in luminosity and/or number density at even moderate redshifts of $z \lesssim 0.5$ (Marzke et al. 1994; Lilly et al. 1995; Ellis et al. 1996; Liu et al. 1998; Bromley et al. 1998; Lin et al. 1999). More recent work has further confirmed and quantified this trend at higher redshifts (see, e.g., Chen et al. 2003; Gabasch et al. 2004; Pérez-González et al. 2005; Dahlen et al. 2005). At low redshifts, evidence is mounting that composite parameterizations may more accurately reflect the shape of the LF than the usual single-function ones (de Lapparent et al. 2003, 2004; Blanton et al. 2005), and that, faintward of $M \sim -18$, the power-law slope of the LF may differ quantitatively from the slope brightward of that threshold (Madgwick et al. 2002; Norberg et al. 2002; Blanton et al. 2005). This could arise, for example, due to large numbers of low-luminosity "blue" galaxies (Wolf et al. 2003) or low surface brightness galaxies (Impey et al. 1996; Blanton et al. 2005) that may have previously evaded detection.

In this paper, we present measurements of the faint-end slopes of the rest-frame V-band luminosity functions of galaxies in the COSMOS survey at $0 \lesssim z \lesssim 0.5$, focusing in particular on the change in that slope as a function of redshift and galaxy spectral type. The depth and breadth of the COSMOS multiband photometry allows for reliable identifications of galaxy redshift and spectral type, with robust redshift error estimates for each galaxy, to a limit of $m_{\rm AB} \sim 25$ in the optical passbands. Even so, the relatively large and varying redshift uncertainties of photometric redshifts can present substantial quantitative challenges and systematic biases (SubbaRao et al. 1996; Liu et al. 1998; Chen et al. 2003; Dahlen et al. 2005). We use Monte Carlo simulations to characterize these biases and to recover the faint-end slopes of galaxy-type–specific LFs.

This work represents an initial study of the general properties of these type-specific faint-end LF slopes, to provide quantitative comparisons with the results of other large field galaxy surveys. Studies of the bright-end evolution of the galaxy LF from the COSMOS survey are given elsewhere (e.g., Scarlata et al. 2007), and a more detailed breakdown of the $0 \lesssim z \lesssim 0.5$ galaxy population by redshift, galaxy spectral type, and galaxy morphology will be presented in a future paper (C. Liu et al. 2008, in preparation). Throughout this paper, we adopt a flat cosmology with $\Omega_\Lambda = 0.7$, $\Omega_m = 0.3$, and $H_0 = 70$ km s^{-1} Mpc^{-1}.

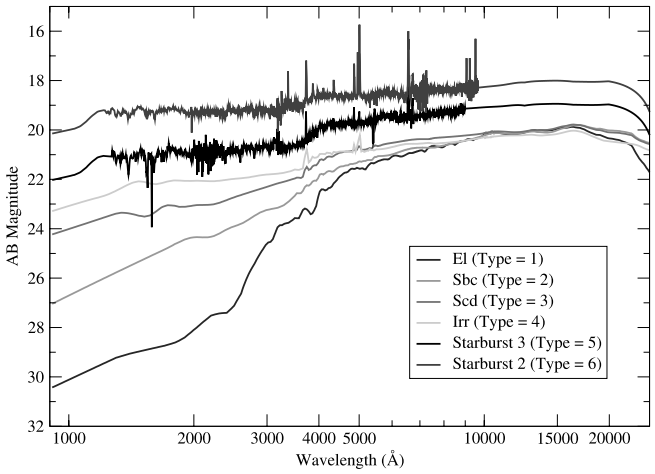

FIG. 1.—Spectral energy distributions from Mobasher et al. (2007) used to compute COSMOS galaxy spectral types and photometric redshifts. This figure is a reproduction of Fig. 1 of Mobasher et al. [*See the electronic edition of the Journal for a color version of this figure*.]

2. GALAXY SAMPLE AND PHOTOMETRIC REDSHIFTS

In our analysis, we use a compilation of the COSMOS optical/near-infrared data (Capak et al. 2007; Mobasher et al. 2007), which includes observations with the *HST* ACS (I_{814}), the Subaru Telescope (B, V, r', i', z', and NB816), the Canada-France-Hawaii Telescope (CFHT; u^* and i^*), and the 4 m KPNO Mayall and CTIO Blanco Telescopes (K_s), as well as supplementary data from the Sloan Digital Sky Survey. The data from the different telescopes were all matched to a common pixel scale and smoothed to the same point-source function. SExtractor (Bertin & Arnouts 1996) was then used in dual mode to generate a photometric catalog, selected using the Subaru i' and CFHT i^* images. The limiting 3 σ AB magnitude is $i' = 26.03$. A detailed description of the imaging data, photometry, and photometric calibration is given in Capak et al. (2007).

Photometric redshifts for individual galaxies were computed using the methods described in Mobasher et al. (2007). Six basic galaxy spectral types adapted from the four template types (E, Sbc, Scd, and Im) from Coleman et al. (1980) and the starburst templates SB2 and SB3 of Kinney et al. (1996) were used. These templates are presented graphically in Figure 1. These galaxy spectral types are derived from empirical data and represent the range of non-AGN galaxy spectral energy distributions (SEDs) from redder to bluer colors; these starburst SEDs, for example, represent very blue galaxies not significantly reddened or obscured by dust. Interpolation was used between the six spectral types to produce a grid of 31 possible galaxy SED fits.

Using the multiband photometry, the COSMOS photometric redshift code (Mobasher et al. 2007) was used to derive a photometric redshift z_p for each galaxy, with 68% and 95% confidence intervals computed above and below that value. To determine the accuracy of the code, the z_p-values were compared

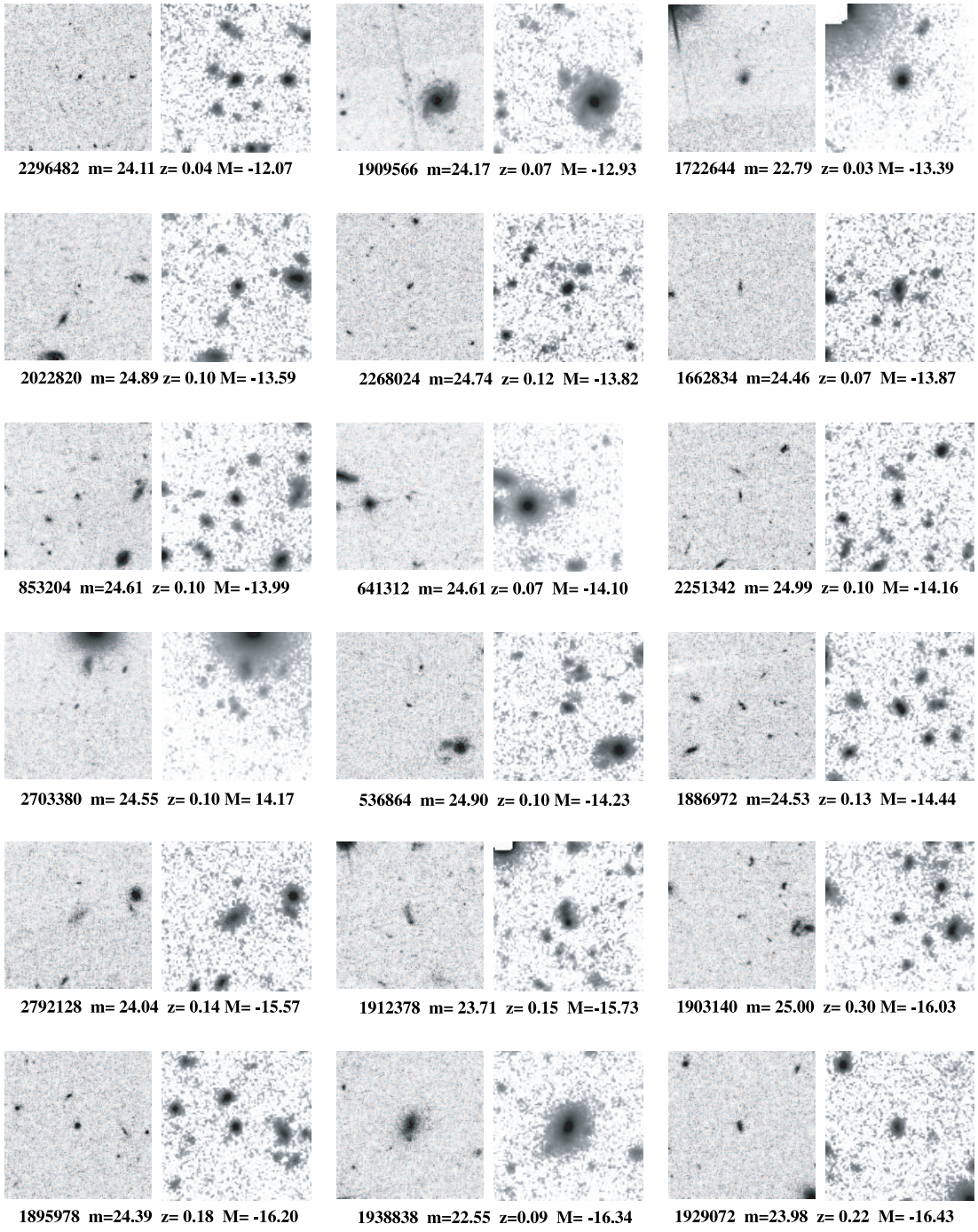

FIG. 2.—*HST* ACS I_{814} and Subaru B images of a representative selection of very low luminosity galaxies in the COSMOS field. Each image is 15″ across, and each image pair is labeled by the COSMOS catalog ID number, photometric redshift, and apparent and absolute V magnitudes of the object at the image center.

with spectroscopic redshifts (z_s) in 868 galaxies with $z < 1.2$ and $i_{AB} \lesssim 24$ that had secure redshift measurements from the zCOSMOS survey (Lilly et al. 2007). The galaxy spectral types (20% early-type, 63% spiral, and 17% starburst) are evenly distributed with redshift in the spectroscopic sample, and about half of the sample (45%) is at $z_s \leq 0.5$.

The detailed statistics of the z_p and z_s comparisons are described in Mobasher et al. (2007), primarily in terms of the parameter $\Delta z = (z_p - z_s)/(1 + z_s)$. As given in Table 4 and Figure 5 of Mobasher et al. (2007), the nominal dispersion between these photometric redshifts and spectroscopically determined redshifts was rms(Δz) = 0.033 for non-AGN galaxies. With respect to the different spectral types, Mobasher et al. (2007) showed that early-type, spiral, and starburst galaxies have values of rms(Δz) = 0.034, 0.030, and 0.042, respectively.

We chose to compute our luminosity functions using the V-band data for this study. The saturation limit for bright objects in that image was $V \sim 18.5$, and the 3 σ faint-detection limit was $V \sim 26.4$, so we conservatively chose as our apparent magnitude range $19.0 < m_V < 25.0$. Details of the photometry are described in Capak et al. (2007). An extinction-corrected, rest-frame absolute M_V magnitude based on the derived z_p and using the K-correction for the best-fit spectral type was computed for each galaxy. Ground- and space-based images of a representative subsample of the faintest galaxies ($M_V \sim -16$ and fainter) in this sample are presented in Figure 2.

3. LUMINOSITY FUNCTIONS

As with all surveys that rely primarily on photometric rather than spectroscopic redshifts, the application of the COSMOS galaxy sample to the derivation of galaxy LFs requires great care in order to account for both random and systematic errors in the redshift determinations. Just as methods of computing photometric redshifts have evolved and improved (Koo 1986; Connolly et al. 1995; Liu & Green 1998; Benítez 2000; Mobasher et al. 2004, 2007), so too have the techniques with which to quantify and compensate for the effects of relatively large redshift error bars in LF calculations (SubbaRao et al. 1996; Liu et al. 1998; Chen et al. 2003; Dahlen et al. 2005; Pérez-González et al. 2005).

In this work, we adapt the method used in Liu et al. (1998), updating it with additional components similar to those used in more recent studies (e.g., Chen et al. 2003; Dahlen et al. 2005; Pérez-González et al. 2005) to reproduce the faint-end slope of the LFs of COSMOS galaxies. Our strategy is based on the $1/V_{\rm max}$ method (Schmidt & Green 1986), which is well described by Chen et al. (2003) as a maximum likelihood method with which to estimate a luminosity function without assuming any parametric form. We account for photometric redshift errors by weighting the galaxies as probability-smoothed luminosity distributions at the redshifts where they are measured.

3.1. *The Modified* $1/V_{\rm max}$ *Method*

Consider a galaxy with an apparent magnitude of m_f in a passband f and with a redshift of $z \pm \sigma$. If $\sigma = 0$, then the absolute magnitude is

$$M_f = m_f - 5\log\,[d_L(z)] - 25.0 - k_f(z),$$

where $d_L(z)$ is the luminosity distance in units of Mpc and $k_f(z)$ is the K-correction at that redshift, in that passband, for the spectral energy distribution of the galaxy. The contribution of that galaxy to the luminosity distribution is then a delta function of amplitude unity at redshift z.

In the case in which $\sigma > 0$ and the error distribution is Gaussian, the galaxy can be thought of as adding a series of fractional contributions to the luminosity distribution in the redshift space surrounding z. Such a fraction at, for example, redshift $z + \delta z$ and with a differential redshift width of dz would have an absolute magnitude of

$$M_f' = m_f - 5\log\,[d_L(z+\delta z)] - 25.0 - k_f(z+\delta z)$$

and an amplitude of

$$N_{z+\delta z} = \frac{P_{\rm G}(z+\delta z,\, z,\, \sigma)\, dz}{A_{\rm G}(z+\delta z,\, z,\, \sigma)},$$

where $P_{\rm G}$ and $A_{\rm G}$ are the Gaussian probability function and its integral, respectively (see, e.g., Bevington & Robinson 1992).

For the photometric redshifts of the COSMOS survey, the redshift error distribution is not Gaussian, but rather can be modeled as two half-Gaussians (Capak et al. 2007; Mobasher et al. 2007), where the 68% confidence interval on the lower and upper limits are σ_l and σ_u, respectively. For a galaxy with a photometric redshift z_p, the amplitude of each fractional contribution to the luminosity distribution would be

$$N_{z+\delta z} = \frac{P_{\rm G}(z+\delta z,\, z,\, \sigma_l)\, dz}{A_{\rm G}(z+\delta z,\, z,\, \sigma_l)}$$

for $z < z_p$ and

$$N_{z+\delta z} = \frac{P_{\rm G}(z+\delta z,\, z,\, \sigma_u)\, dz}{A_{\rm G}(z+\delta z,\, z,\, \sigma_u)}$$

for $z > z_p$.

This "fuzzing" of a galaxy's luminosity distribution in redshift space is straightforwardly achieved numerically, with a choice of $dz \ll \sigma$ to minimize random magnitude errors. For this COSMOS data set, we used $dz_l = 0.02\sigma_l$ and $dz_u = 0.02\sigma_u$. This divides each galaxy into a Gaussian-weighted luminosity distribution with 300 bins from $z - 3\sigma_l$ to $z + 3\sigma_u$. The entire distribution for each galaxy is normalized to unity.

In the standard $1/V_{\rm max}$ method, each galaxy contributes a weight to the luminosity function that is equal to the inverse of the accessible volume within which it can be observed. The accessible volume, referred to here as $V_{\rm max}$, is the total comoving volume within the redshift boundaries of the sample in which the given galaxy could be and fall within the selection criteria of the sample. In our case, the relevant criteria are the bright and faint apparent magnitude limits and the effective solid angle of the COSMOS survey.

In the case of a probability-weighted luminosity distribution for individual objects, it is straightforward to compute $V_{\rm max}$ for each fractional galaxy; correspondingly, its contribution to the luminosity function is $(1/V_{\rm max})N_{z+\delta z}$. Assembling the luminosity function is then a matter of summing those contributions within absolute magnitude bins.

3.2. *Redshift Limits and Sample Size*

Since the primary goal of this work was to examine the LF faint-end slope, the upper redshift boundary was determined mainly by our desire to sample with high completeness to at least as faint as $M_V \sim -16.5$ in the entire redshift range. For a typical galaxy in the sample, depending on the galaxy's K-correction, this corresponds roughly to $z \lesssim 0.4$. But because each galaxy's luminosity is calculated as a probability-weighted distribution, there is a statistically significant contribution to the LF at more than a full magnitude beyond the formal absolute magnitude limit. Thus, with the caveat that we are beyond that limit, we were also able to derive faint-end slopes of the LFs of galaxies in the redshift range $0.4 < z \leq 0.5$.

Similarly, in the low-redshift range, we are also able to measure fainter in absolute magnitude than the formally faintest detectable galaxy. However, to avoid large systematic magnitude errors and biases from structure in the local universe, we set a lower redshift bound of $z > 0.02$ for deriving the LFs. This means that we have statistically meaningful luminosity contributions to the LFs down to an absolute magnitude of $M_V \sim -12.8$ for $0.02 < z \leq 0.1$.

Within our apparent magnitude limits of $19.0 < V < 25.0$, the COSMOS survey photometric and z_p catalog (Capak et al. 2007) contains 49,161 galaxies in the redshift range $0.02 < z \leq 0.5$. Below and above this redshift range, however, there are galaxies within the apparent magnitude limits whose probability-smoothed luminosity distributions contribute to the light within that range. Using δ_{68} to denote the width of the 68% confidence interval for z_p, we thus also include the contributions of all other galaxies whose luminosity distribution tails fall within $3\delta_{68}$. (For example, a galaxy with $z_p = 0.51$ and $\delta_{68} = 0.05$ would contribute the portion of its luminosity distribution from the range $0.36 \leq z \leq 0.50$, while a galaxy with $z_p = 0.61$ and $\delta_{68} = 0.05$ would contribute from the range $0.46 \leq z \leq 0.50$.) There are 31,659 galaxies in the catalog that make such a partial contribution;

TABLE 1
Galaxy Samples and z_p Confidence Levels

Number of Galaxies	Redshift Constraints	δ_{68} Constraints[a]	Median $\delta_{68}/(1+z)$	Mean $\delta_{68}/(1+z)$	rms $\delta_{68}/(1+z)$
41,237	...	≤ 0.1	0.042	0.041	0.053
49,161	$0.02 \leq z \leq 0.50$	...	0.043	0.050	0.073
80,820	...	...	0.052	0.081	0.239

Note.—Galaxy spectral types as defined by Mobasher et al. (2007).
[a] The quantity δ_{68} is the width of the 68% confidence interval for z_p.

even though many of those galaxies add only a tiny fraction of a galaxy into the $z \leq 0.5$ redshift range, we include them in our analysis for statistical completeness. Thus, a total of 80,820 galaxies are included in the sample used to derive the LFs.

To check how the inclusion of these galaxies might affect the distribution of the z_p accuracy in the sample as a whole, we created a subset of the 80,820 galaxy sample in which the galaxies have a value of δ_{68} of at most 0.1. This subset of 41,237 galaxies (51% of the entire sample) effectively contains objects whose values of δ_{68} are no more than 3 times the rms(Δz) of the spectroscopically tested accuracy of the COSMOS z_p code. We then computed the mean, median, and rms values of $\delta_{68}/(1+z)$ for the 41,237, 49,161, and 80,820 galaxy samples. We give the results in Table 1. As might be expected, the median, mean, and rms values all increase as the constraints in redshift and δ_{68} are lifted and the sample sizes grow. The median $\delta_{68}/(1+z)$ value increases only modestly on an absolute numerical basis (from 0.042 to 0.043 to 0.052); the mean and rms values increase more substantially.

3.3. *Simulations*

Computing LFs using "fuzzy" galaxies with photometric redshifts is clearly vulnerable to a set of systematic errors that would not be present for a galaxy sample with secure spectroscopic redshifts. In this work, we use the standard galaxy LF parameterization of Schechter (1976), where M^* is the characteristic magnitude, ϕ^* is the characteristic number density, and α is the faint-end slope (Lin et al. 1996):

$$\phi(M) = \phi^*(0.4 \ln 10) \exp\left(-10^{-0.4(M-M_*)}\right) 10^{-0.4(M-M_*)(1+\alpha)}\, dM. \quad (1)$$

In any given redshift bin, objects near the peak of the LF—that is, near M^*—will have part of their light distributed toward brighter magnitudes, and objects at the bright and faint ends of the galaxy sample will have their light scattered still further. This will cause an overestimate of those parts of the LF that contribute the least light. In addition, as the luminosity contributions of the galaxies are distributed across a large redshift range, light from galaxies inside a given redshift bin will sometimes be scattered out of that bin, and since lower z redshift bins have smaller volumes than higher z ones, there is the risk that more light would be added into lower redshift bins than would be removed from them. This could bias the distribution of derived absolute magnitudes in those bins.

We quantify and correct for these errors using Monte Carlo simulations in the manner described by Liu et al. (1998). For an arbitrary fixed M^* and ϕ^*, we created populations of galaxies that followed Schechter functions with faint-end slopes in the range $-2.2 < \alpha < -0.2$. For each value of α, we populated a simulated COSMOS survey volume with the corresponding galaxy population. We then "detected" these galaxies on the basis of the magnitude and redshift limits of our survey, and for each galaxy detected, we randomly added an error to the redshift of that galaxy that was consistent with the measured dispersion of the COSMOS photometric redshift catalog, rms(Δz) = 0.033. Finally, we assigned to that galaxy a value of δ_{68} equal to the median value of δ_{68} of the 80,820 galaxy sample; i.e., $0.052(1+z_s)$. The LF for this simulated galaxy sample was then computed using the modified $1/V_{\max}$ method described above.

We generated 150 such simulated LFs for each value of α tested. To illustrate the results of these simulations, we present three sets of them in Figure 3. The dashed lines show the input faint-end slopes ($\alpha = -0.7$, -1.1, and -1.5) for the simulations. Of the 150 simulations, we exclude the four outliers furthest above and four furthest below the input value of α; the remaining 142 simulations (i.e., 95%) yield results that fall within the envelope bounded by the solid lines above and below each dashed line. The values of α represented by each of those solid and dashed lines are given in the figure.

As Figure 3 shows, the "fuzzing" of the galaxies due to z_p uncertainties does cause systematic biases of the calculated faint-end LF slope. At $\alpha \simeq -1.1$, the bias is negligible, and the fuzzing basically just increases the uncertainty of the measured slope. For steeper input values of α, however, the output value of α is quantitatively biased toward steeper values, and for shallower input values of α, the opposite is true. The bias increases as the input values of α grow more extreme; an input of $\alpha = -1.9$, for example, produces output values of α in a 95% envelope in the range $-2.3 \lesssim \alpha \lesssim -1.8$, whereas an input of $\alpha = -0.4$ produces a corresponding output of $-0.5 \lesssim \alpha \lesssim +0.1$.

From all the simulation results, standard bootstrap methods were used to estimate the expected systematic offsets in α for an

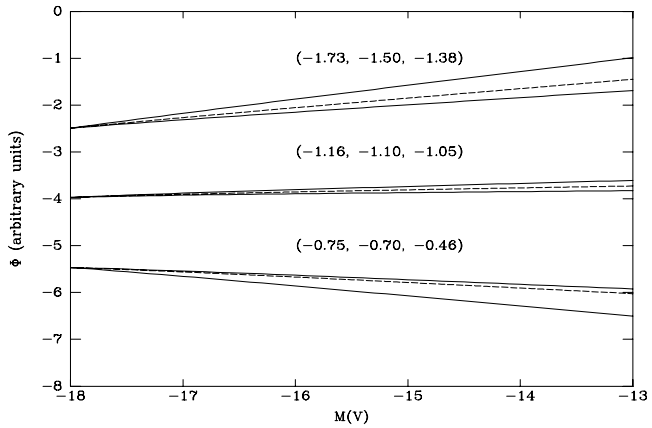

Fig. 3.—Examples of the results of simulations testing the biasing effect of probability-weighted luminosity functions on the measurement of α. The dashed lines represent the α-values of the input LFs, and the solid lines show the boundaries wherein 95% of the output LFs are contained. The three numbers above each set of lines are the α-values of the upper bound, input, and lower bound LFs, respectively.

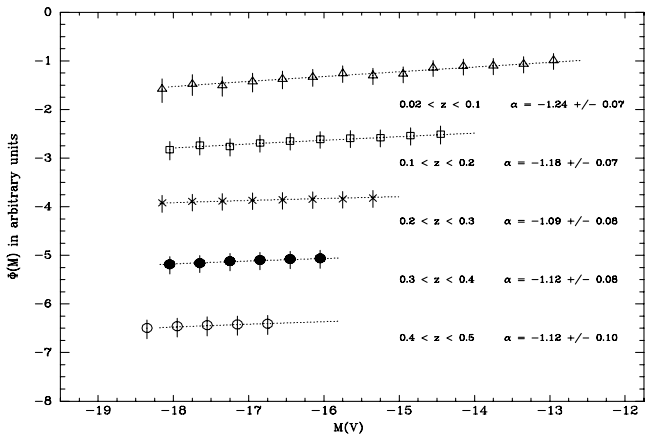

FIG. 4.—Faint-end portions of the *V*-band galaxy luminosity functions, $\Phi(M_V)$, in the redshift range $0.02 \leq z \leq 0.5$. Each LF is offset by a constant for clarity. The best-fit weighted least-squares faint-end power-law slope for each LF has been overplotted (*dotted lines*) and is labeled with its redshift bin and slope.

actually observed galaxy population. These offsets were then used to correct the computed luminosity functions in order to recover the original faint-end slopes of the galaxy samples in each redshift bin. This correction affects the overall slope only and is not intended to remove any inherent, non–power-law structure in the observed LF. Also, this correction strategy was optimized to recover the faint-end slope, rather than the characteristic magnitude M^* or the number density normalization ϕ^* (as was done, for example, in Chen et al. 2003). We thus do not attempt to measure those parameters in this work. Accurate measurement of those values for the COSMOS survey are presented, for a slightly different galaxy spectral type classification scheme, by Scarlata et al. (2007).

3.4. *Probability-weighted Luminosity Functions*

The measured luminosity functions for the entire galaxy sample, corrected for this bias in α, are presented in Figure 4. Only the faint ends of the LFs, operationally defined here as galaxies fainter than $M_V \simeq -18$, are presented. LFs were calculated in five redshift bins: $0.02 < z \leq 0.1, 0.1 < z \leq 0.2, 0.2 < z \leq 0.3$, $0.3 < z \leq 0.4$, and $0.4 < z \leq 0.5$. In addition, we divided the galaxies into four subsamples according to galaxy spectral type: type 1 (early-type galaxies), type 2 (Sbc), types 3 and 4 combined (Scd + Irr), and types 5 and 6 combined (low-extinction starbursts). For each subsample, LFs were also calculated in the same five redshift bins. The results are presented in Figure 5.

There are three primary sources of errors in the LFs: (1) the systematic error in the LF slope and absolute magnitude determinations, described in the text above and characterized using simulations; (2) a Poisson-like error that derives naturally from the modified $1/V_{\max}$ method, which is the reciprocal of the square root of the total number of fractional galaxies in each bin; and (3) a non-Gaussian error as a function of absolute magnitude, due to the asymmetric uncertainty in the photometric redshift determination of each galaxy. The second source of error, because of our large galaxy sample size, is much smaller than the third source of error. We computed the error from that third source with a standard bootstrap technique, using 150 random samplings

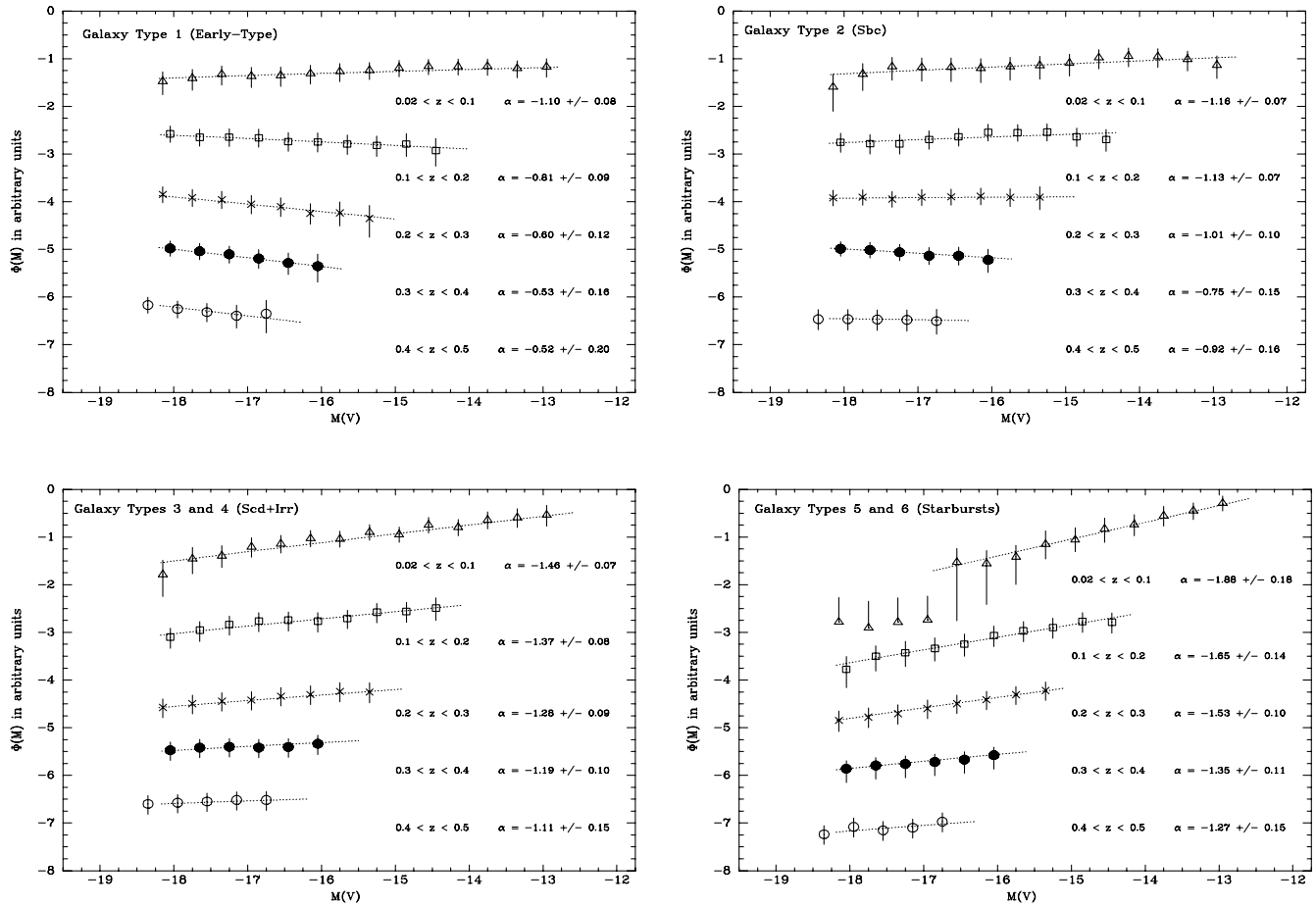

FIG. 5.—Faint-end portions of *V*-band luminosity functions, $\Phi(M_V)$, for galaxies divided by spectral type. Symbols are the same as those in Fig. 4.

TABLE 2
Luminosity Function Slope Fits

Galaxy Spectral Type[a]	Redshift Range	α
T1–T6 (All)	$0.02 \leq z < 0.1$	-1.24 ± 0.07
	$0.1 \leq z < 0.2$	-1.18 ± 0.07
	$0.2 \leq z < 0.3$	-1.09 ± 0.08
	$0.3 \leq z < 0.4$	-1.12 ± 0.08
	$0.4 \leq z < 0.5$	-1.12 ± 0.10
T1 (early-type)	$0.02 \leq z < 0.1$	-1.10 ± 0.08
	$0.1 \leq z < 0.2$	-0.81 ± 0.09
	$0.2 \leq z < 0.3$	-0.60 ± 0.12
	$0.3 \leq z < 0.4$	-0.53 ± 0.16
	$0.4 \leq z < 0.5$	-0.52 ± 0.20
T2 (Sbc)	$0.02 \leq z < 0.1$	-1.16 ± 0.07
	$0.1 \leq z < 0.2$	-1.13 ± 0.07
	$0.2 \leq z < 0.3$	-1.01 ± 0.10
	$0.3 \leq z < 0.4$	-0.75 ± 0.15
	$0.4 \leq z < 0.5$	-0.92 ± 0.16
T3 + T4 (Scd + Irr)	$0.02 \leq z < 0.1$	-1.46 ± 0.07
	$0.1 \leq z < 0.2$	-1.37 ± 0.08
	$0.2 \leq z < 0.3$	-1.28 ± 0.09
	$0.3 \leq z < 0.4$	-1.19 ± 0.10
	$0.4 \leq z < 0.5$	-1.11 ± 0.15
T5 + T6 (starbursts)	$0.02 \leq z < 0.1$	-1.88 ± 0.18
	$0.1 \leq z < 0.2$	-1.65 ± 0.14
	$0.2 \leq z < 0.3$	-1.53 ± 0.10
	$0.3 \leq z < 0.4$	-1.35 ± 0.11
	$0.4 \leq z < 0.5$	-1.27 ± 0.15

[a] Galaxy spectral types as defined by Mobasher et al. (2007).

(with duplication allowed) of the observed data set to determine the 68% confidence intervals for Φ in each magnitude bin.

Each LF segment was fitted to a power-law slope using weighted least squares. To avoid possible biasing of the faint-end slope by galaxies near M^*, which as we mentioned above is not well determined by our technique, we only use data fainter than $M_V = -18.3$ in our fits. In one case, we make a more restrictive magnitude cutoff: the lowest redshift bin in the starburst spectral type. There the measured LF drops discontinuously at $M_V = -17$. We suspect that this has occurred because M^* may be quite faint for this galaxy type and redshift bin, thus distorting our measurement of the LF brightward of that point. So to ensure that the α fit to that LF is not correspondingly distorted, we use only data fainter than $M_V = -16.8$ for that particular fit. In both Figures 4 and 5, the measured LF data points are plotted as symbols, and the best-fit α-values are plotted as dotted lines. The faint-end slope fits are summarized in Table 2.

4. DISCUSSION

Because of the combined large area and depth of the COSMOS survey, the luminosity functions presented in this work provide a glimpse of α across a substantial range of redshift in a single, consistent data set. With this view, our results show that for all spectral types combined, $\alpha = 1.24 \pm 0.07$ for the local ($0.02 < z \leq 0.1$) universe. As the redshift increases, α flattens out somewhat, and it is -1.12 ± 0.10 in our highest redshift bin ($0.4 < z \leq 0.5$).

Our local LF is consistent with results from the two largest local galaxy surveys to date, which have comparable ($\sim 10^5$ galaxies) sample sizes to our study here. The 2dFGRS survey found that, for the b_J-band galaxy luminosity function, $\alpha = -1.21 \pm 0.03$ (Norberg et al. 2002), and it was -1.18 ± 0.02 for the redshift range $0.02 < z < 0.25$ (Croton et al. 2005). The SDSS has $\alpha = -1.05 \pm 0.01$ for a slightly redshifted r-band galaxy LF for galaxies brighter than $M_r \sim -17$ (Blanton et al. 2003) and $\alpha \simeq -1.3$ at fainter magnitudes (Blanton et al. 2005). Blanton et al. (2005) have further shown that, with the appropriate conversion of the 2dFGRS b_J data, they and the SDSS g-band LFs have consistent low-luminosity slopes. At higher redshift, our results are consistent with those of Scarlata et al. (2007), who independently derived $\alpha = -1.26 \pm 0.15$ in the range $0.2 < z < 0.4$ for a portion of the COSMOS survey area. Our results are also consistent with results from other surveys given in the literature; for example, with the V-band LF derived from the VIRMOS-VLT Deep Survey (VVDS; Ilbert et al. 2005), where $\alpha = 1.21 \pm 0.04$ in the range $0.2 < z < 0.4$.

The formal errors in our α measurements are higher than those of most of these other studies; this is probably mainly because of the systematic slope uncertainties that we attempt to account for with our simulations. Our overall agreement, however, appears to confirm that we have properly accounted for the errors that result from representing galaxies as probability-smoothed luminosity distributions.

4.1. *LFs as a Function of Galaxy Spectral Type*

The luminosity functions in the four galaxy spectral type bins we used—SED templates of early-type, Sbc, Scd+Irr, and low-extinction starbursts—follow the well-known pattern of steeper values of α for bluer galaxies. In our low-redshift bin, α increases from -1.10 ± 0.08 in early types to -1.88 ± 0.18 in starbursts; the trend continues with increasing redshift, showing a similar steepening of α from -0.52 ± 0.20 to -1.27 ± 0.15.

As with the full galaxy sample, these type-specific results are consistent with the findings of previous work in the literature. Of course, due to differing galaxy selection criteria and redshift binning, exact comparisons are not always possible. Generally speaking, however, for local galaxies, our red/early-type and intermediate spiral galaxy LFs are consistent with SDSS and 2dFGRS results, and previous samples of $z \lesssim 0.1$ galaxy populations have also shown very steep values of α for the bluest and most irregular galaxies: $\alpha = -1.87$ for the CfA Redshift Survey (Marzke et al. 1994), -1.84 for the Las Campanas Redshift Survey (Bromley et al. 1998), -1.81 for the SSRS2 (Marzke et al. 1998), and -1.9 from the Deep Multicolor Survey (Liu et al. 1998) and the SDSS (Nakamura et al. 2003). At higher redshifts, comparisons with COMBO-17 (Wolf et al. 2003), the VVDS (Zucca et al. 2006), and the COSMOS survey itself (Scarlata et al. 2007) show broad consistency across the various galaxy type and redshift intervals.

4.2. *α versus z: Evolution or Selection?*

In the context of the broad consistency of our results with those in the literature, perhaps the most striking result in this work is the clear trend, with every galaxy spectral type, of a flattening of the faint-end slope with increasing redshift. From our lowest redshift bin to our highest—i.e., from $z \sim 0$ to $z \sim 0.5$—the change in slope $\Delta\alpha = 0.58$, 0.24, 0.35, and 0.61, respectively, for early types, Sbc, Scd+Irr, and low-extinction starbursts.

On the surface, this trend may not appear to be consistent with previous work. Much of the work to derive the evolution of the galaxy LF parameters M^* and Φ^* as a function of redshift (e.g., Lin et al. 1999; Wolf et al. 2003; Baldry et al. 2005; Willmer et al. 2006) in fact depends on the assumption that α does not evolve with redshift, or at most weakly evolves to $z \lesssim 1$. We have focused here on the measurement of α rather than those other parameters; that, and the fact that all of our measurements have

come from a single data set, plus the fact that each individual determination of α is consistent with previous work, supports the likelihood that this observed flattening trend is real.

The question is, do these changing slopes represent true evolution in α, or do they reflect our ability to detect different galaxy populations as a function of redshift? The latter possibility can be discussed in the context of, among others, de Lapparent et al. (2003) and Blanton et al. (2005), who suggest that the faint end of the field galaxy LF is comprised of a composite population of dwarf and nondwarf galaxies, each with its own functional form. This would mean that a single power law is not quite sufficient to describe the LF faint end accurately. Blanton et al. (2005) further suggest, through detailed examination of the faint galaxy population in the SDSS, that a large fraction of these dwarf galaxies may have very low surface brightnesses and are thus not included in most faint-end LF measurements.

Our dependence on photometric redshifts places an important caveat on the interpretation of our data: by using "fuzzy" galaxies, any second-order deviations from a power law at the faint end of the LF may well have been smoothed out and are thus not recoverable from our LF measurements. So if a deviation from a single faint-end power law does occur at very low luminosities, we cannot address that issue with this work.

Due to the substantial depth of the COSMOS survey imaging, it is likely that we have successfully measured a larger fraction of low surface brightness dwarf galaxies than have wider area, shallower surveys such as SDSS or 2dFGRS. The steepness of our low-redshift LFs may reflect this. Even the COSMOS survey depth, however, does not allow us to measure values of α fainter than $M_V \sim -17$ at $z = 0.5$, so we cannot say if the flattening of α in our higher redshift bins is due to the nondetection of these dwarfs. There may be some circumstantial evidence, however, to support that picture. For example, Dahlen et al. (2005) measured for the GOODS survey a value of $\alpha = -1.37$ for the rest-frame B band in the range $0.1 < z < 0.5$, which is somewhat steeper than most LF measurements in this range. However, the GOODS survey is very deep, so in this broad redshift bin, a large detected fraction of faint, low surface brightness dwarfs near $z \gtrsim 0.1$ could have driven α to a steeper value for the full range.

When the spectroscopic portion of the COSMOS survey (Lilly et al. 2007) is completed, we will be able to address this question in more detail, as we deconvolve the faint end of the galaxy LF as a multivariate function of color, morphology, luminosity, and redshift.

5. CONCLUSIONS

Using the COSMOS multiband photometry and photometric redshift catalog, we have constructed faint-end rest-frame V-band luminosity functions for the galaxy population at $0.02 < z \leq 0.5$ in the COSMOS survey volume. Since we are using photometric redshifts, we have computed these LFs by treating galaxies as weighted probability-smoothed luminosity distributions and using a modified $1/V_{\rm max}$ method. A total of 49,161 galaxies have photometric redshifts that fall in this redshift range; within and outside this range, a total of 80,820 galaxies contribute to the derived LFs. Extensive Monte Carlo simulations were used to characterize and account for the systematic and random errors of this technique.

For all galaxy spectral types, the LF slope ranges from -1.24 to -1.12 from the lowest redshift bin to the highest. In the lowest redshift bin ($0.02 < z < 0.1$), where the magnitude limit is $M_V \lesssim -13$, the slope ranges from $\alpha = -1.10 \pm 0.08$ for galaxies with early-type spectral energy distributions (SEDs) to $\alpha = -1.88 \pm 0.18$ for galaxies with low-extinction starburst SEDs. In each galaxy SED category (early-type, Sbc, Scd+Irr, and starburst), the faint-end slopes grow shallower with increasing redshift; in the highest redshift bin ($0.4 < z < 0.5$), $\alpha = -0.52 \pm 0.20$ and -1.27 ± 0.15 for early types and starbursts, respectively.

All of our derived type-specific LFs, across our redshift ranges, are broadly consistent with the findings of previous authors. Our results thus show a flattening trend for α with increasing redshift for each spectral type. It is unclear, however, if this is evidence of evolution of α in the galaxy LF or of preferential selection of dwarf galaxies in the local universe. The steepness of α at lower redshift could be qualitatively explained, for example, by large numbers of faint dwarfs, perhaps of low surface brightness, that are not detected at higher redshifts. We will address this question in a future paper, when the full set of COSMOS data, and in particular, spectroscopic redshifts, has been obtained.

The *HST* COSMOS Treasury program was supported through NASA grant HST-GO-09822. We wish to thank Tony Roman, Denise Taylor, and David Soderblom for their assistance in the planning and scheduling of the extensive COSMOS observations. We gratefully acknowledge the contributions of the entire COSMOS collaboration, which contains more than 70 scientists. More information on the COSMOS survey is available at http://www.astro.caltech.edu/~cosmos. It is a pleasure to acknowledge the excellent services provided by the NASA IPAC/IRSA staff (Anastasia Laity, Anastasia Alexov, Bruce Berriman, and John Good) in providing online archive and server capabilities for the COSMOS data sets. The COSMOS Science meeting in 2005 May was supported in part by the NSF through grant OISE-0456439. We thank Paris Bogdanos and James Cohen for image processing and data formatting assistance. C. Liu, T. Paglione, and S. Tribiano gratefully acknowledge support from a City University of New York CCIR grant, as well as the hospitality and support of the Hayden Planetarium and Department of Astrophysics at the American Museum of Natural History.

Facilities: HST (ACS), Subaru, KPNO, CTIO, CFHT.

REFERENCES

Abazajian, K., et al. 2004, AJ, 128, 502
Baldry, I., et al. 2005, MNRAS, 358, 441
Bell, E. F., McIntosh, D. H., Katz, N., & Weinberg, M. D. 2003 ApJS, 149, 289
Benítez, N. 2000, ApJ, 536, 571
Bertin, E., & Arnouts, S. 1996, A&AS, 117, 393
Bevington, P. R., & Robinson, D. K. 1992, Data Reduction and Error Analysis for the Physical Sciences (2nd ed.; New York: McGraw-Hill)
Blanton, M. R., Lupton, R. H., Schlegel, D. J., Strauss, M. A., Brinkmann, J., Fukugita, M., & Loveday, J. 2005, ApJ, 631, 208
Blanton, M. R., et al. 2003, ApJ, 592, 819
Bromley, B. C., Press, W. H., Lin, H., & Kirshner, R. P. 1998, ApJ, 505, 25
Brown, W. R., Geller, M. J., Fabricant, D. G., & Kurtz, M. J. 2001, AJ, 122, 714
Budavari, T., et al. 2005, ApJ, 619, L31
Capak, P., et al. 2007, ApJS, 172, 99
Chen, H.-W., et al. 2003, ApJ, 586, 745
Coleman, G. D., Wu, C.-C., & Weedman, D. W. 1980, ApJS, 43, 393
Colless, M., et al. 2001, MNRAS, 328, 1039
Connolly, A. J., Csabai, I., Szalay, A. S., Koo, D. C., Kron, R. C., & Munn, J. A. 1995, AJ, 110, 2655
Croton, D. J., et al. 2005, MNRAS, 356, 1155
Dahlen, T., Mobasher, B., Somerville, R. S., Moustakas, L. A., Dickinson, M., Ferguson, H. C., & Giavalisco, M. 2005, ApJ, 631, 126
de Lapparent, V., Arnouts, S., Galaz, G., & Bardelli, S. 2004, A&A, 422, 841
Driver, S. P., Popescu, C. C., Tuffs, R. J., Liske, J., Graham, A. W., Allen, P. D., & De Propris, R. 2007, MRAS, 379, 1022

de Lapparent, V., Galaz, G., Bardelli, S., & Arnouts, S. 2003, A&A, 404, 831
Ellis, R. S., Colless, M., Broadhurst, T., Heyl, J., & Glazebrook, K. 1996, MNRAS, 280, 235
Gabasch, A., et al. 2004, A&A, 421, 41
Ilbert, O., et al. 2005, A&A, 439, 863
Impey, C. D., Sprayberry, D., Irwin, M. J., & Bothun, G. D. 1996, ApJS, 105, 209
Kinney, A. L., Calzetti, D., Bohlin, R. C., McQuade, K., Storchi-Bergmann, T., & Schmitt, H. R. 1996, ApJ, 467, 38
Koo, D. C. 1986, ApJ, 311, 651
Lilly, S. J., Tresse, L., Hammer, F., Crampton, D., & Le Fèvre, O. 1995, ApJ, 455, 108
Lilly, S. J., et al. 2007, ApJS, 172, 70
Lin, H., Kirshner, R. P., Shectman, S. A., Landy, S. D., Oemler, A., Tucker, D. L., & Schechter, P. L. 1996, ApJ, 464, 60
Lin, H., Yee, H. K. C., Carlberg, R. G., Morris, S. L., Sawicki, M., Patton, D. R., Wirth, G., & Shepherd, C. W. 1999, ApJ, 518, 533
Liu, C. T., & Green, R. G. 1998, AJ, 116, 1074
Liu, C. T., Green, R. G., Hall, P. B., & Osmer, P. S. 1998, AJ, 116, 1082
Madgwick, D. S., et al. 2002, MNRAS, 333, 133
Marzke, R. O., da Costa, L. N., Pellegrini, P. S., Willmer, C. A., & Geller, M. J. 1998, ApJ, 503, 617
Marzke, R. O., Huchra, J. P., & Geller, M. J. 1994, ApJ, 428, 43
Mobasher, B., et al. 2004, ApJ, 600, L167
———. 2007, ApJS, 172, 117
Nakamura, O., Fukugita, M., Yasuda, N., Loveday, J., Brinkmann, J., Schneider, D. P., Shimasaku, K., & SubbaRao, M. 2003, AJ, 125, 1682
Norberg, P., et al. 2002, MNRAS, 332, 827
Pérez-González, P. G., et al. 2005, ApJ, 630, 82
Scarlata, C., et al. 2007, ApJS, 172, 406
Schechter, P. 1976, ApJ, 203, 297
Schmidt, M., & Green, R. F. 1986, ApJ, 305, 68
Scoville, N. Z., et al. 2007a, ApJS, 172, 1
———. 2007b, ApJS, 172, 38
SubbaRao, M. U., Connolly, A. J., Szalay, A. S., & Koo, D. C. 1996, AJ, 112, 929
Taniguchi, Y., et al. 2007, ApJS, 172, 9
Willmer, C. N. A., et al. 2006, ApJ, 647, 853
Wolf, C., Meisenheimer, K., Rix, H.-W., Borch, A., Dye, S., & Kleinheinrich, M. 2003, A&A, 401, 73
Zucca, E., et al. 2006, A&A, 455, 879